https://doi.org/10.18524/1810-4215.2025.38.340394

ENRICHMENT WITH THE FIRST- AND SECOND-PEAK S-PROCESS ELEMENTS IN GALACTIC DISC GIANTS

T. Mishenina [1], T. Gorbaneva [1], M. Pignatari [2,3,4], T. Kurtukian-Nieto [5]

[1] Astronomical Observatory, Odesa I. I. Mechnikov National University, 1v Marazliivska St, Odesa, 65014, Ukraine, *tmishenina@ukr.net*

[2] Konkoly Observatory, HUN-REN, Konkoly-Thege Miklós út 15-17, Budapest 1121, Hungary

[3] MTA Centre of Excellence, Konkoly-Thege Miklós út 15-17, Budapest 1121, Hungary

[4] E. A. Milne Centre for Astrophysics, University of Hull, Cottingham Rd, Hull HU6 7RX, UK

[5] Instituto de Estructura de la Materia, C. de Serrano, 113 bis-119-121-123, Madrid E-28006, Spain

ABSTRACT. The distribution patterns of chemical elements in the Galactic disc remain insufficiently described. In particular, despite considerable attention to the enrichment of disc stars with neutron-capture elements, several questions remain unresolved and warrant further investigation.

In this study, we examine the enrichment of disc stars with first- and second-peak slow neutron-capture (s-process) elements using a sample of 150 Galactic disc giants. Their spectra were obtained with the 1.93-m telescope at the Observatoire de Haute-Provence (France), using the ELODIE echelle spectrograph.

Elemental abundances of the first-peak (Sr, Y, Zr) and second-peak (Ba, La, Ce) s-process elements were determined using synthetic spectrum fitting under the assumption of Local Thermodynamic Equilibrium (LTE). The results were compared with predictions from Galactic Chemical Evolution (GCE) models.

Our findings confirm that the enrichment in both first- and second-peak s-process elements is driven by contributions from both the s-process and r-process, with a possible additional input from other nucleosynthesis sources.

Keywords: stars: abundances – stars: atmospheres – stars: stellar evolution.

АНОТАЦІЯ. Моделі хімічної еволюції Галактики, що враховують внесок кількох поколінь зір та різних подій нуклеосинтезу, зазвичай використовуються для визначення збагачення та походження хімічних елементів у Галактичному диску. Однак ми все ще маємо недостатнє відтворення спостережуваних проявів збагачення та розподілу елементів у диску. Зокрема, незважаючи на значну увагу до питань, пов'язаних зі збагаченням зір диска елементами, утвореними в процесах захоплення нейтронами, питання все ще залишаються, і це потребує подальшого розгляду. У цій роботі ми досліджуємо збагачення зір диска елементами 1-го та 2-го піків повільного захоплення нейтронів, так званого s-процесу, спираючись на вибірку з 150 гігантів Галактичного диска. Використовувалися спектри зір-гігантів, отримані за допомогою 1,93-метрового телескопа Обсерваторії Верхнього Провансу (Франція) і ешельного спектрографа ELODIE, що охоплюють діапазон довжин хвиль 4400–6800 Å з роздільною здатністю R = 42 000 та співвідношенням сигнал/шум від 130 до 230 при 5500 Å. Вміст елементів першого (Sr, Y, Zr) та другого (Ba, La, Ce) піків s-процесу було отримано методом синтетичного спектру в припущенні Локальної Термодинамічної Рівноваги (ЛТР). Отримані дані порівнюються з моделями Галактичної хімічної еволюції (ГХЕ). Наші результати підтверджують, що збагачення елементів 1-го та 2-го піків s-процесу зумовлене як s-процесом, так і r-процесом (швидким захопленням нейтронів), не виключаючи також додаткового внеску інших джерел нуклеосинтезу.

Ключові слова: зорі: вміст – зорі: атмосфера – зорі: еволюція зір.

1. Introduction

Modern models of the chemical evolution of the Galaxy at disc metallicities account for contributions from multiple generations of stars and incorporate various enrichment sources. However, they still fall short of fully reproducing observational data, leaving several key aspects of elemental enrichment insufficiently explained. It is generally accepted that first-peak slow neutron-capture (s-process) elements – such as strontium (Sr), yttrium (Y), and zirconium (Zr) – are primarily produced in the ejecta of massive asymptotic giant branch (AGB) stars, whereas second-peak elements – such as barium (Ba), lanthanum (La), and cerium (Ce) – are mainly contri buted by low-mass AGB stars. This leads to a relative enhancement of first-peak elements around [Fe/H] ≈ –2 and of second-peak elements around [Fe/H] ≈ –1.5.

Despite significant progress in modeling and observations, the enrichment of Galactic disc stars with

Table 1: Comparison of obtained stellar parameters with those reported by other authors for the N stars common to our sample.

Reference	ΔT_{eff} (K)	Δlogg (dex)	ΔV_t (km/s)	Δ[Fe/H] (dex)	**N**
Tautvaišienė et al. 2021	–32 ±86.70	–0.30 ± 0.29	–	–0.02 ± 0.09	88
Forsberg et al. 2019	–10.56 ±57.03	–0.32 ± 0.08	0.00 ± 0.12	0.03 ± 0.05	89

neutron-capture elements (particularly those formed via the s-process) still presents unresolved questions. In this study, we address these issues by analyzing the abundances of first- and second-peak s-process elements in a sample of 150 disc giant stars.

2. Observations and atmospheric parameters

The spectra were observed with the 1.93-m telescope at Observatoire de Haute-Provence (France) using the ELODIE echelle spectrograph covering 4400–6800 Å at a resolving power of R = 42,000, with signal-to-noise ratios of 130 to 230 at 5500 Å. The initial data reduction followed Katz et al. (1998), and further analysis (continuum normalisation, equivalent width measurement, etc.) was conducted with the DECH30 software developed by G. Galazutdinov (http://gazinur.com/DECH-software.html).

To determine the effective temperature Teff, we used the calibrations of the dependence of line intensities on Teff obtained in the work of Kovtyukh et al. (2006), with the mean random error of a single calibration being 65–70 K (45–50 K in most cases and 90–95 K in the least accurate cases). The use of about 70–100 calibrations per spectrum reduces the uncertainty to 5–7 K. Spectroscopic determinations of the gravity log g by two methods were used: 1) a method of iron ionization equilibrium, where the average iron abundance determined from Fe I lines and Fe II lines must be identical, and 2) a method that relies on the detailed wing fitting of the Ca I 6162 Å line. Turbulent velocity V_t is determined by the independence of the iron content determined for a given line from its equivalent width. The metallicity [Fe/H] is adopted as the iron abundance determined from the Fe I lines. The more details and comparisons with results of other authors, see Mishenina et al. (2006).

In this work, we compared the parameter values with those obtained in recent works by Tautvaishiene et al. (2021) and Forsberg et al. (2019), as shown in Table 1. For more details and comparisons with results of other authors, see Mishenina et al. (2006).

The errors of the log g determination for giants are about 0.2-0.3 dex as indicated in Mishenina et al. (2006). The comparison of our atmospheric parameters with the results of Tautvaishiene et al. (2021) and Forsberg et al. (2019) estimated that the accuracy of our parameter determinations is as follows: ΔT_{eff} =±100 K, surface gravities Δlogg =±0.3 dex and microturbulent velocity ΔV_t =±0.1 km/s.

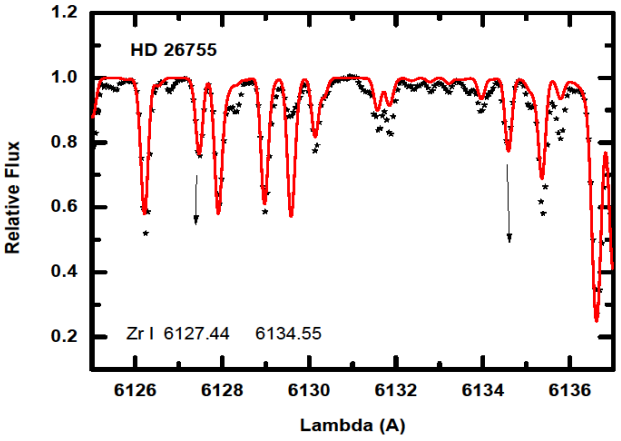

Figure 1: Spectrum synthesis fitting of the Zr lines to the observed profiles.

3. Abundance and age determinations

The Sr, Zr, Ba, La, Ce abundances were derived using the Local Thermodynamical Equilibrium (LTE) approach applying the models of Castelli & Kurucz (2004) and the modified STARSP LTE spectral synthesis code (Tsymbal, 1996). The oscillator strengths log gf were adopted from the last version of the VALD data base (Kupka et al., 1999). Hyperfine structure and isotopic composition were considered for Ba and La. Yttrium abundances were taken from Mishenina et al. (2007). Adopted solar abundances follow Asplund et al. (2009). Typical abundance uncertainties from atmospheric parameters are ~0.15 dex for all elements.

Stellar ages were estimated using the [Y/Mg] vs. age calibration (see, e.g. Tucci Maia et al. 2016), based on Mg and Y abundances taken from Mishenina et al. (2006; 2007).

4. Results and discussions

We investigated the abundances of six elements formed via neutron-capture processes: strontium (Sr), yttrium (Y), and zirconium (Zr), classified as first-peak s-process elements, and barium (Ba), lanthanum (La), and cerium (Ce), associated with the second peak. To facilitate comparative analysis, we calculated the mean abundances for each group: $\langle[El/Fe]\rangle_{1\text{-st}}$ = ([Sr/Fe] +

[Y/Fe] + [Zr/Fe]) / 3 (first peak) and $\langle[El/Fe]\rangle_{2\text{-nd}}$ = ([Ba/Fe] + [La/Fe] + [Ce/Fe]) / 3 (second peak).

We then plotted the average abundance of the first-peak elements against that of the second-peak elements.

Figure 2 displays a correlation between these two datasets, with a Pearson correlation coefficient of r = 0.656, indicating a moderate linear relationship, underlining that AGB star contributions dominate the sample. But not a direct proportionality suggests that the two groups of elements may originate from distinct nucleosynthetic processes.

This result may support the prevailing hypothesis that first-peak elements are predominantly synthesized in moderately massive AGB stars (4–7 $M_\odot$), while second-peak elements are mainly produced in low-mass AGB stars (1–3 $M_\odot$), indicating different sources of enrichment. However, the absence of a strict linear proportionality implies the possible involvement of other production mechanisms associated with massive stars, e.g. such as core-collapse supernovae (CCSNe), the weak s–process (Pignatari et al., 2010), or such as the νp-process contributions by Fröhlich et al. (2006) as well as the neutrino wind contributions by Arcones & Thilemann (2013) etc.

Figure 3 presents the difference between the average abundances of the second- and first-peak elements, normalized to the first-peak mean. The plot reveals a weak correlation and a broad scatter of data points. If AGB stars dominate, their difference between second peak and first peak contributions should be close to constant, independent of the abscissa coordinate. This is what was found in Fig.3, combined with a large scatter.

In contrast, Figure 4, which shows the difference between the first- and second-peak average abundances relative to the second-peak mean, exhibits a clearer correlation with a Pearson coefficient of r = 0.85. This can be interpreted as the contribution of massive stars minus AGB stars vs. the contribution of AGB stars. If AGB stars dominate, then as their contribution increases, this difference should obviously decrease, leading to a moderately strong negative linear relationship between both quantities, as we can be seen in Fig. 4 (with a Pearson correlation coefficient of -0.85).

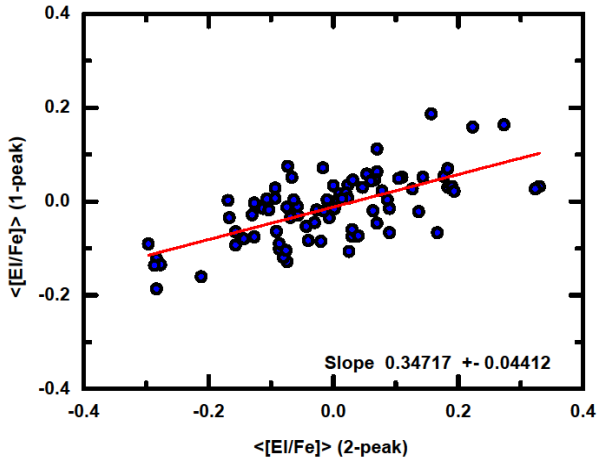

Figure 2: Dependences of the average abundance of the 1-st s-process peak relative to the 2-nd-peak average.

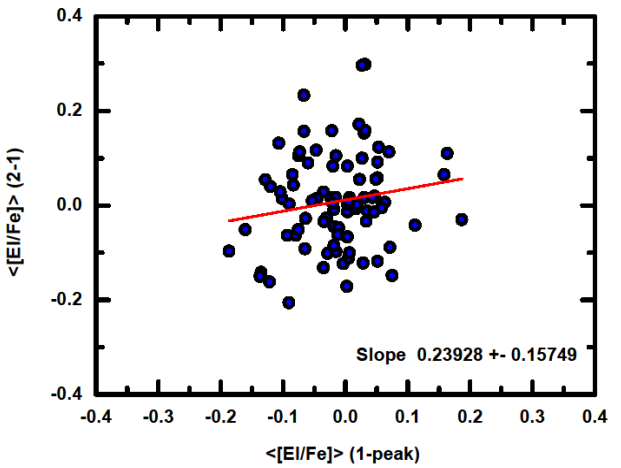

Figure 3: Difference between the average abundances of the 2-nd and 1-st s-process peaks relative to the 1-st-peak average.

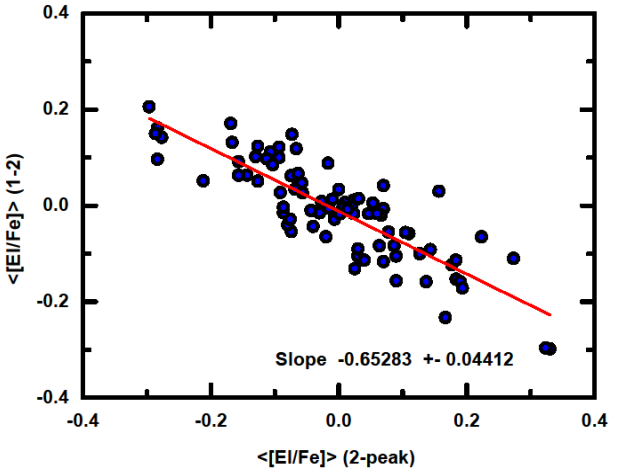

Figure 4: Difference between the average abundances of the 1-rst and the 2-nd peaks relative to the 2-nd peak average.

Both figures (3 and 4) further support the view that these two groups of elements originate from different stellar sources, and suggest a non-negligible role of additional enrichment processes.

Figure 5 illustrates the relationship between the average abundances of first- and second-peak elements and stellar age. Although no strong trends are apparent, the second-peak elements show a notably larger scatter. This may reflect differences in production sources or inherent uncertainties in abundance determinations. However, the uncertainties are comparable across all studied elements, which implies that the observed scatter is likely of astrophysical origin. If the larger scatter in second peak elements is not due to uncertainties in abundance determinations, it might reflect the metallicity dependence of a secondary s-process behaviour in AGB stars combined with the fact that lower metallicities lead to a larger neutron/Fe seed ratio and consequently to an abundance pattern shifted towards heavy elements.

For stars with near-solar metallicity, direct comparison with individual nucleosynthesis models becomes

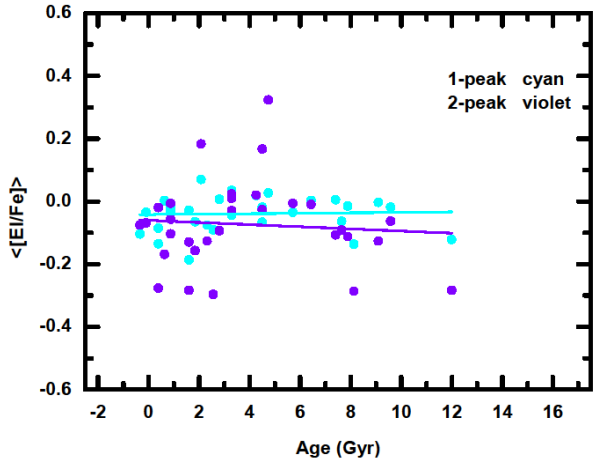

Figure 5: Dependence of the average abundances of the first- and second-peak s-process elements on stellar age.

challenging due to cumulative enrichment from multiple stellar generations. In such cases, Galactic Chemical Evolution (GCE) models are used to trace enrichment sources. These models incorporate parameters such as the initial mass function (IMF), stellar yields from different mass ranges, star formation rates, and timescales of chemical enrichment.

Our preliminary analysis suggests that GCE models must account for the relative contributions of low- and intermediate-mass AGB stars, as well as potential input from other nucleosynthetic sources, to adequately reproduce the observed abundance patterns of s-process elements.

To interpret our results, we compared the observed abundances with GCE model predictions developed by Kobayashi et al. (2020). These models incorporate multiple nucleosynthesis sources: The s-process from AGB stars based on yields from Karakas & Lugaro (2016) for metallicities Z = 0.007, 0.014, and 0.03). Additional contribution besides iron: ECSNe (high-mass super-AGB stars that explode as electron-capture supernovae) using yields from Wanajo et al. (2013).

The r-process (rapid neutron capture) from various sources: ν-driven winds (Arcones et al. 2007; Wanajo 2013, and their calculations of SN II), NS-NS/NS-BH (neutron stars, black hole) mergers (the nucleosynthesis yields from the 3D-GR calculation of a NS-NS merger ($1.3M_{\odot}$+$1.3M_{\odot}$) from Wanajo et al. (2013) both for NS-NS and NS-BH mergers, and MRSNe – supernovae with strong magnetic field (e.g. Nishimura et al., 2015).

Figures 6–8 show the comparison between observed and model-predicted abundances of the first-peak elements Sr, Y, and Zr. The dashed lines represent models with the s-process from AGB stars only, while the solid lines include additional contributions from ECSNe, NS–NS/NS–BH mergers, and MRSNe. As noted by the model authors: "The first peak elements, Sr, Y, and Zr, are sufficiently produced by ECSNe together with AGB stars." We would note, however, that at these metallicities we expect rather the weak s-process is produced by massive supernovae CCSNe (Pignatari et al. 2010) than by ECSNe.

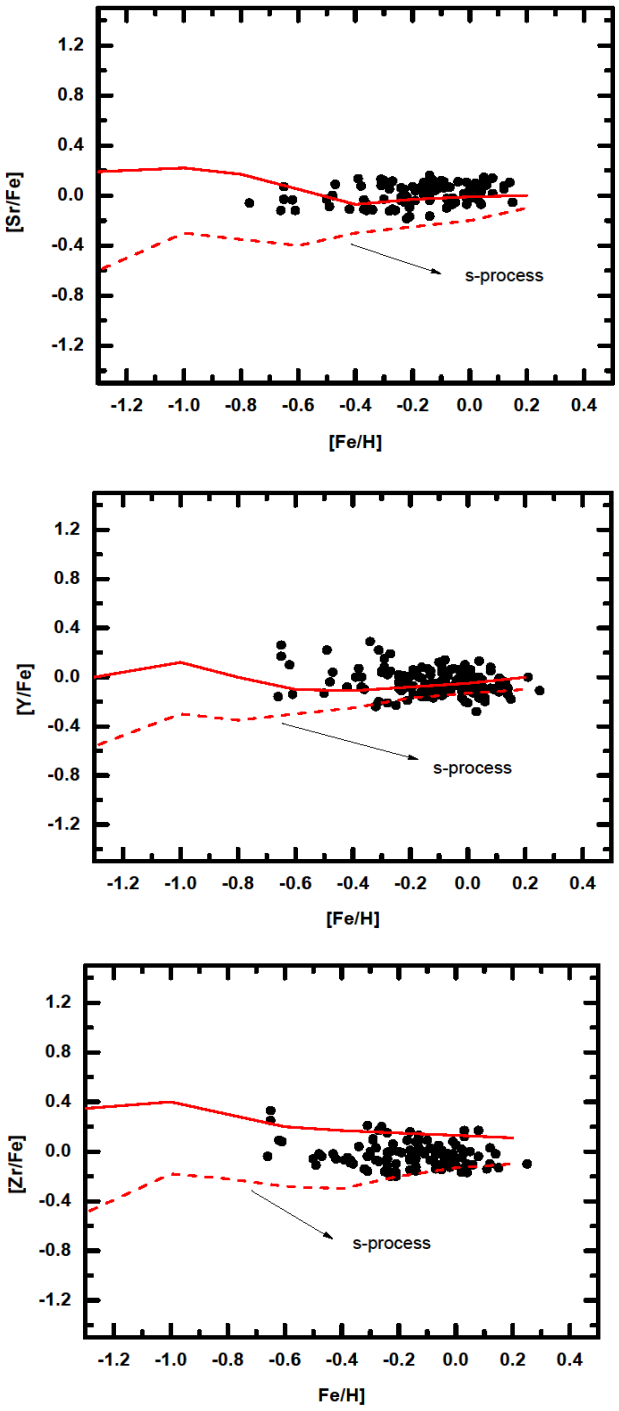

Figures 6, 7, 8: [Sr/Fe], [Y/Fe], [Zr/Fe] vs. [Fe/H] and model tracks from Kobayashi et al. (2020).

Figures 9–11 show model comparisons for the second-peak elements Ba, La, and Ce. For Ba, the s-process from AGB stars alone matches the observed data well. For La and Ce, however, the model predictions slightly overestimate the observed abundances. This discrepancy may indicate that the adopted yields require refinement–either in the stellar source parameters or in the modeling of neutron-producing reactions.

These comparisons reinforce our earlier observational findings, particularly the differences in behavior between first- and second-peak elements, and support the conclusion that multiple nucleosynthesis processes–

beyond the classical s-process–contribute to the chemical enrichment of the Galactic disc.

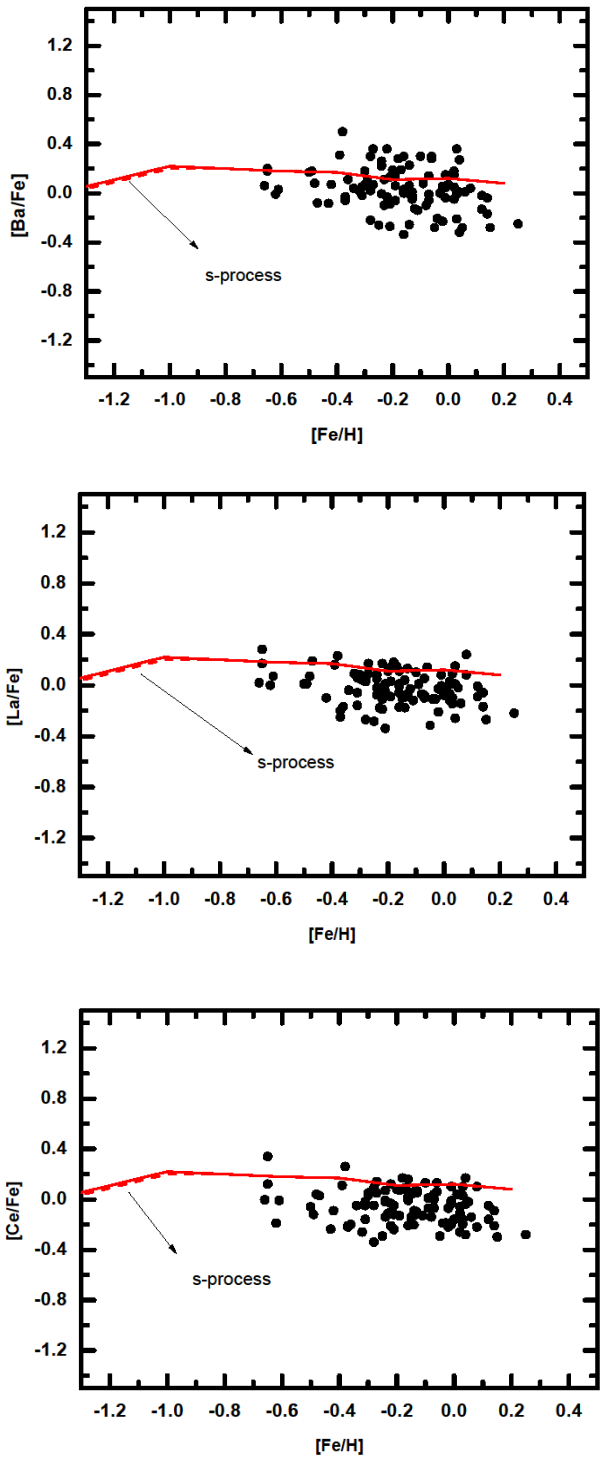

Figures 9, 10, 11: [Ba/Fe], [La/Fe], [Ce/Fe] vs. [Fe/H] and model tracks from Kobayashi et al. (2020).

5. Conclusions

1. We studied abundances of Sr, Y, Zr, Ba, La, and Ce for a sample of 150 giant stars in the Galactic disc.
2. A moderate linear correlation (Pearson's coefficient r = 0.656) was found between the average abundances of first- and second-peak s-process elements. However, the lack of direct proportionality indicates contributions from distinct nucleosynthesis processes, and possibly additional production channels.
3. Comparisons with Galactic Chemical Evolution (GCE) models support our observational results. While the models can explain some trends (especially for Ba), they also highlight the need to refine yield predictions and better understand the contributions of different nucleosynthetic sources.
4. Our findings underscore the complexity of neutron-capture element production in the Galactic disc and emphasize the need for further theoretical modeling and high-precision observational data to better constrain the origins of both first- and second-peak s-process elements.

Acknowledgements. We express our deepest gratitude to the referee for their careful reading of the manuscript and a number of valuable comments that significantly improved the work. We kindly acknowledge the support of the project "Stellar Nucleosynthesis in Advanced Burning Phases and Explosive Scenarios, 2024-2027" of the Institute of the Structure of Matter (Instituto de Estructura de la Materia), Madrid, Spain.

References

Arcones A., Janka H.-Th., Scheck L.: 2007, *A&A*, **467**, 1227.
Arcones A., Thielemann F.-K.:2013, *JPhysG,* **40**, id. 013201
Asplund M., Grevesse N., Sauval A. J., Scott P.: 2009, *ARA&A*, **47**, 481.
Castelli F., Kurucz R.: 2004, *ArXiv Astrophysics e-prints astro-ph/0405087*
Galazutdinov G.: http://www.gazinur.com/DECH-software.html
Forsberg R., Jonsson R., Ryde N., Matteucci F.: 2019, *A&A*, **631**, 113.
Fröhlich C., Martínez-Pinedo, G, . Liebendörfer, M. et al.: 2006*, PRL,* **96,** id. 142502
Karakas A. I., Lugaro M.: 2016, *ApJ*, **825**, 26.
Katz D., Soubiran, C., Cayrel R. et al.: 1998, *A&A*, **338**, 151.
Kobayashi C., Karakas A.I., Lugaro M.: 2020, *ApJ*, **900**, 179.
Kovtyukh V., Soubiran C., Bienaymé O. et al.: 2006, *MNRAS*, **371**, 879.
Kupka F., Piskunov N., Ryabchikova T. et al.: 1999, *A&AS*, **138**, 119.
Mishenina T., Bienaymé O., Gorbaneva T. et al.: 2006, *A&A*, **456**, 1109.
Mishenina T., Gorbaneva T., Bienaymé O. et al.: 2007, *ARep*, **51**, 382.
Nishimura N., Takiwakai T., Thielemann F.-K.: 2015, *ApJ*, **810**, 109.
Pignatari M., Galino R., Heil M. et al.: 2010, *ApJ,* **710**, 1557.
Tautvaišienė G., Viscasillas Vázquez C., Mikolaitis Š. et al.: 2021, *A&A*, **649**, A126.
Tsymbal V.: 1996, *ASPC*, **108**, 198.
Tucci Maia M., Ramírez I., Meléndez J. et al.: 2016, *A&A*, **590**, A32.
Wanajo S.: 2013, *ApJ*, **770**, L22.
Wanajo S., Janka H.-T., Müller B.: 2013, *Ap*J, **767**, L26.